Crystallographic cut that maximizes of the birefringence in photorefractive crystals

Corte cristalográfico que maximiza la birrefringencia en cristales fotorrefractivos

Jorge Enrique Rueda-Parada
Ph. D. Natural Science, Physic
Universidad de Pamplona
Pamplona, Colombia
jorgeenriquerueda@gmail.com

Resumen– **La birrefringencia por efecto electro-óptico depende del tipo de cristal, del corte del cristal, del campo eléctrico aplicado y de la dirección de incidencia de la luz sobre las caras principales del cristal. Se presenta un estudio de maximización de la birrefringencia en cristales fotorrefractivos de simetría cristalográfica cúbica, en términos de estos tres parámetros. Expresiones analíticas generales para la birrefringencia fueron obtenidas, a partir de las cuales se puede establecer la birrefringencia de cualquier tipo de corte. Un nuevo corte cristalográfico fue encontrado, cuyo valor de birrefringencia es mayor que los cortes comerciales PROM, PRIZ y HUIGNARD.**

Palabras clave– **Cristales fotorrefractivos; Birrefringencia; Efecto electro-óptico.**

Abstract– **The electro-optical birefringence effect depends on the crystal type, cut crystal, applied electric field and the incidence direction of light on the principal crystal faces. It is presented a study of maximizing the birefringence in photorefractive crystals of cubic crystallographic symmetry, in terms of these three parameters. General analytical expressions for the birefringence were obtained, from which birefringence can be established for any type of cut. A new crystallographic cut was encountered; the birefringence value is greater than PROM, PRIZ and HUIGNARD commercial cuts.**

Keywords– **Photorefractive crystals; Birefringence; electro-optical effect.**

1. INTRODUCTION

The photorefractive crystals are light modulators, electro-optical and photoconductive, and have optical memory [5],[12],[13]. These materials are of particular interest related to dynamic holography and optical amplification applications, between others [4]-[7], [9]-[21]. The optical efficiency of these materials depends on the direction of light propagation through the birefringence of the same material, and the applied electric field [5],[12]. The crystal cut refer to the principal crystal faces, each of which is parallel to a particular crystallographic plane. Thus, each cut corresponds to a maximum birefringence and thus a maximum optical efficiency. Using the numerical Newton-Raphson method [8] was determined the cut that maximizes the birefringence in cubic crystals with 3m23 symmetry. The methodology can be applied to other crystallographic symmetries. The results were compared with the birefringence in PROM, HUIGNARD and PRIZ commercial cuts [4]-[7].

2. SOLUTION OF THE PROBLEM

The solution of the problem from the mathematical model of index ellipsoid [1], defined by (1):

$$\sum_{i,j=1}^{3} \left(n_{ij}^{-2} x_1 x_j \delta_{ij} + \Delta B_{ij} x_i x_j \right) = 1 \quad (1)$$

where the first term of this equation represents the undisturbed state of the crystal, and second term is the ΔB_{ij} disturbed state. The n_{ij} parameter is the refractive index tensor, and $x_{i,j}$ are spatial coordinates. With $\delta_{ij}=0$ if $i \neq j$, and $\delta_{ij}=1$ if $i=j$. Figure.1 is a scheme that defines index ellipsoid. It is presented the solution for the particular case of isotropic crystals ($n_{11}= n_{22}= n_{33}= n_o$) [1],[2], that exhibit electro-optic effect of the first order, where the perturbation (electro-optic effect) is given by (2):

$$\Delta B_{ij} = \sum_{k=1}^{3} \gamma'_{ijk} E_k \qquad j = 1,..,6 \qquad (2)$$

Where γ'_{ijk} is the electro-optic tensor (EOT) in the proper axes system of the crystal, and E_k is the electric field applied perpendicularly to principal faces crystal.

Fig.1. INDEX ELLIPSOID. THE x_1, x_2, x_3 ARE PROPER AXES (PERPENDICULAR TO (HKL) CUT PLANES). THE x'_1, x'_2, x'_3 ARE AXES PARALLEL TO NEUTRAL LINES OF THE CRYSTAL. THE n_1, n_2, n_3 ARE PRINCIPAL REFRACTIVE INDICES. THE X,Y,Z ARE CRYSTALLOGRAPHIC AXES

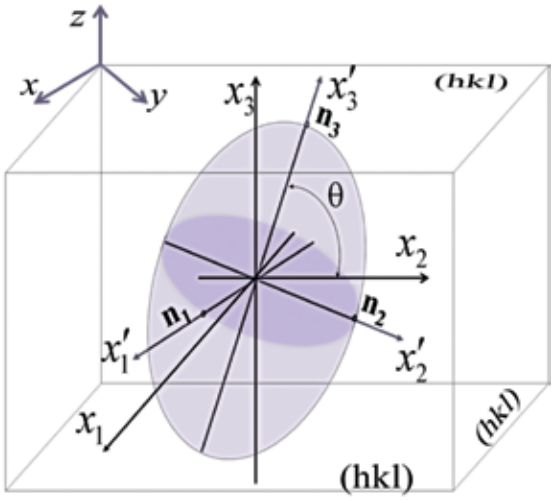

Fuente: autor.

In equation (3), the r_{lmn} electro-optic tensor is given in the (x,y,z) system. This transformation is applied when the proper axes are not parallel to (x,y,z) axes:

$$r'_{ijk} = \sum_{l,m,n=1}^{3} a_{il} a_{jm} a_{kn} r_{lmn} \qquad (3)$$

where i,j,k = 1..3, and $a_{il,jm,kn}$ are the coefficients of the transformation R(α,β,γ) matrix as a function of the Euler angles [3]. These angles define the crystal cut. Also in (3), due to symmetry of the EOT can be applied the next contraction of indexes (4):

$$\begin{aligned} r_{1k} &= r_{11k} \quad r_{4k} = r_{32k} = r_{23k} \\ r_{2k} &= r_{22k} \quad r_{5k} = r_{13k} = r_{31k} \\ r_{3k} &= r_{33k} \quad r_{6k} = r_{21k} = r_{12k} \end{aligned} \qquad (4)$$

Then, eighteen terms of electro-optical tensor are obtained in the system of proper axes. For the particular study of this work, the non-zero and equal terms are $r_{41} = r_{52} = r_{63}$. This tensor is given in a (x,y,z) system, axes parallel to the [100], [010], [001] crystallographic directions. The birefringence can be calculated from equation (1) given in the proper axes system of the crystal:

$$\begin{aligned} &n_0^{-2}(x_1^2 + x_2^2 + x_3^2) + \Delta B_1 x_1^2 + \Delta B_2 x_2^2 \\ &+\Delta B_3 x_3^2 + 2\Delta B_4 x_2 x_3 + 2\Delta B_5 x_1 x_3 \\ &+2\Delta B_6 x_1 x_2 = 1 \end{aligned} \qquad (5)$$

Equation (5), it can be considered three illumination directions perpendicular to the (h,k,l) planes cut (Fig.1):

Case 1. Illumination parallel to the x_1 axes:

$$\begin{aligned} &(n_0^{-2} + \Delta B_2) x_2^2 + (n_0^{-2} + \Delta B_3) x_3^2 \\ &+2\Delta B_4 x_2 x_3 = 1 \end{aligned} \qquad (6)$$

Case 2. Illumination parallel to the x_2 axes:

$$\begin{aligned} &(n_0^{-2} + \Delta B_1) x_1^2 + (n_0^{-2} + \Delta B_3) x_3^2 \\ &+2\Delta B_5 x_1 x_3 = 1 \end{aligned} \qquad (7)$$

Case 3. Illumination parallel to the x_3 axes:

$$\begin{aligned} &(n_0^{-2} + \Delta B_1) x_1^2 + (n_0^{-2} + \Delta B_2) x_2^2 \\ &+2\Delta B_6 x_1 x_2 = 1 \end{aligned} \qquad (8)$$

Equations (6) to (8) represent indices planes parallel to the $(0,x_2,x_3)$, $(x_1,0,x_3)$ and $(x_1,x_2,0)$ crystal faces, respectively. Moreover, the equations (6) to (8) have the form (9),

$$Ax_i^2 + Cx_j^2 + Bx_i x_j = 1 \qquad (9)$$

with $i \neq j$, and $B \neq 0$, and where:

$$Tan(2\theta) = \frac{B}{A - C} \qquad (10)$$

We can assume that the proper axes do not coincide with neutral lines, and then it facilitates to find general expressions for the birefringence. These solutions must be transformed to coordinates of the neutral lines. Assuming that the neutral lines are rotated to an θ angle with relation to its proper axes, then (11):

$$\begin{aligned} &\left(A\cos^2\theta + C\sin^2\theta + \frac{B^2}{2\sqrt{B^2 + (A-C)^2}}\right) X_i'^2 + \\ &\left(A\sin^2\theta + C\cos^2\theta - \frac{B^2}{2\sqrt{B^2 + (A-C)^2}}\right) X_j'^2 = 1 \end{aligned} \qquad (11)$$

Coefficients of the (11) define the n_i and n_j principal indices refraction, thus:

$$n_i = \frac{1}{\sqrt{A\cos^2\theta + C\sin^2\theta + \frac{B^2}{2H}}} \qquad (12)$$

$$n_j = \frac{1}{\sqrt{A\sin^2\theta + C\cos^2\theta - \frac{B^2}{2H}}} \qquad (13)$$

Where $n_i = n_2$ and $n_j = n_3$ for Case 1; $n_i = n_1$ and $n_j = n_3$ for Case 2; $n_i = n_1$ and $n_j = n_2$ for Case 3; with $H = \sqrt{B^2 + (A-C)^2}$. If (12) and (13) are expanded into Taylor series, then we can obtain:

$$n_i = C^{-1/2} - \frac{C^{-3/2}}{4}\left[(A-C) + \sqrt{(A-C)^2 + 4B^2}\right] \quad (14)$$

$$nj = C^{-1/2} - \frac{C^{-3/2}}{4}\left[(A-C) + \sqrt{(A-C)^2 + 4B^2}\right] \quad (15)$$

$$\delta n = |n_i - n_j| = \frac{C^{-3/2}}{2}\sqrt{(A-C)^2 + B^2} \quad (16)$$

Table I contains general expressions obtained for the birefringence and the orientation of the neutral lines.

TABLE I

GENERAL SOLUTIONS POCKELS BIREFRINGENCE IN ISOTROPIC CRYSTALS

PROPAGATION	Tan (2θ)	BIREFRINGENCE
$\overrightarrow{k_{x1}}$	$\frac{2\Delta B_4}{\Delta B_2 - \Delta B_3}$	$\delta n_{23} = \frac{n_0^3}{2}\sqrt{(\Delta B_2 - \Delta B_3)^2 + 4\Delta B_4^2}$
$\overrightarrow{k_{x2}}$	$\frac{2\Delta B_5}{\Delta B_1 - \Delta B_3}$	$\delta n_{13} = \frac{n_0^3}{2}\sqrt{(\Delta B_1 - \Delta B_3)^2 + 4\Delta B_5^2}$
$\overrightarrow{k_{x3}}$	$\frac{2\Delta B_6}{\Delta B_1 - \Delta B_2}$	$\delta n_{12} = \frac{n_0^3}{2}\sqrt{(\Delta B_1 - \Delta B_2)^2 + 4\Delta B_6^2}$

3. ALGORITHM OF THE NUMERICAL METHOD AND RESULTS

With these before expressions, we can calculate the birefringence of the crystal. The following is the algorithm for the numerical calculations:

1. Define a cut: R(α,β,γ).
2. Calculate r'_{ijk}.
3. Calculate the perturbation with three field components, equation (2).
4. Calculate the birefringence (for each interest case of the Table 1).
5. Check if the birefringence is the maximum, then finishes.

In the birefringence numerical maximization process, we can use the three equations of birefringence (Table I). The other part, It was used as input parameters, the EOT of a BSO crystal (r_{41}=4 pm/V) and three electric field components. The Newton-Raphson routine seeks maximum birefringence between the three expressions of the Table I, and in terms of the cut angle defined by [α;β;γ]. The software system output reports the cut angles [α;β;γ], the elements of the perturbation vector, and r'_{ijk}. Equations (17) to (19) are results of numerical maximization of the birefringence process.

$$\gamma' = \gamma_{41} 10^{-4} x \begin{bmatrix} 7947 & 71 & 136 \\ -3332 & -3055 & 7133 \\ -4612 & -4048 & -849 \\ -2235 & 7133 & -4048 \\ 136 & -2235 & -4612 \\ 7103 & -3332 & -2235 \end{bmatrix} \quad (17)$$

$$\delta n_{JERP} = \frac{n_0^3 r_{41}}{2}\sqrt{\left(\sum_{j=1}^{3}(T_{1j} - T_{3j})E_j\right)^2 + 4\left(\sum_{j=1}^{3} T_{5j}E_j\right)^2} \quad (18)$$

$$Tan(2\theta) = \frac{2x\sum_{j=1}^{3} T_{5j}E_j}{\sum_{j=1}^{3}(T_{1j} - T_{3j})E_j} \quad (19)$$

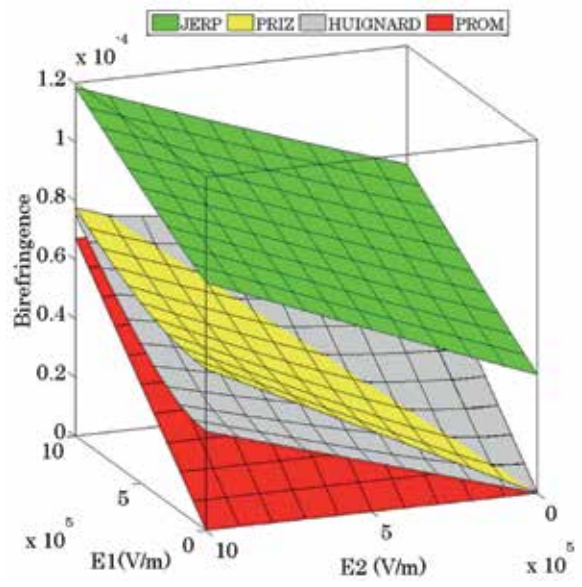

Fig. 2. BIREFRINGENCE BEHAVIOR OF THE PROM, PRIZ, HUIGNARD CUTS AND NEW JERP CUT FOUND [α=24°1';β=119°6'; γ=30°22']. WITH $E_1=E_2=E_3$ = 1x10^6 V/m, no=2.56, r_{41}=4 pm/V

Fuente: autor.

TABLE II

RELATIONSHIP BETWEEN BIREFRINGENCE JERP CUT RELATED TO BIREFRINGENCE OF THE PRIZ, HUIGNARD AND PROM CUTS. THE CONDITIONS OF ELECTRIC FIELD (FIRST COLUMN) WERE APPLIED ONLY IN THE CALCULATION OF δJERP.

ELECTRIC FIELD	BIREFRINGENCE	
$E_1, E_2, E_3 \neq 0$	δJERP =	1.53×δPRIZ 1.58×δHUIGNARD 1.77×δPROM
$E_1=0$ and $E_2, E_3 \neq 0$		1.09×δPRIZ 1.12×δHUIGNARD 1.25×δPROM
$E_2=0$ and $E_1, E_3 \neq 0$		1.01×δPRIZ 1.04×δHUIGNARD 1.17×δPROM
$E_3=0$ and $E_1, E_2 \neq 0$		1.03×δPRIZ 1.06×δHUIGNARD 1.19×δPROM

The maximization algorithm was implemented in Fortran, where $1x10^{-6}$ rad precision was used to the [α;β;γ] angles. We found that the birefringence is maximum for [α=24°1'; β=119°6'; γ=30°22'] cut, with the light propagation on the k_{x2} direction. The equations (18) and (19) are the maximum birefringence and orientation of the neutral lines, respectively. Fig. 2 shows the numerical results of birefringence found with related to PROM, PRIZ, and HUIGNARD traditional cuts, and new cut (JERP). Table II contains the birefringence of the new cut compared with the traditional cuts.

4. CONCLUSIONS

It has been maximized the birefringence of photorefractive materials, in terms of the cutting of the principal crystal faces. It has been encountered a new cut, which was evaluated for four directions of the applied electric field, and the three main directions of propagation of light in the crystal. In all cases tested, the birefringence of the new cut is greater than PROM, PRIZ, and HUIGNARD commercial cuts. Furthermore, the general analytical expressions of birefringence were found. From these new expression can be studied, with less difficulty, analytically or numerically any birefringence crystal cubic crystallographic structure.

REFERENCES

[1] I. P. Kaminow, E. H. Turner, "Electrooptic Light Modulators", *Appl. Opt*., 5, 10, 1966.

[2] J. Nye, "*Proprietés Physiques de Cristaux"*, Ed. Masson, 1985.

[3] H. Goldstein, J. Safko, "*Classical Mechanics"*, Third Edition, Addison-Wesley (2002).

[4] S. Hou, D. Oliver, Pockels Readout Memory Using BSO, *App. Lett.,* 18, 325, 1971.

[5] J. Huignard, F. Micheron, "High-sensitivity read-write volume $Bi_{12}SiO_{20}$ and $Bi_{12}GeO_{20}$ crystal", *App.Phys. Lett.,* 29, 591, (1976).

[6] D. Casasent, F. Caimi, A. Khomenko, "Soviet Priz spatial light modulator", *App. Opt*., 20, 4215, 1981.

[7] D. Casasent, F. Caimi, M. P. Petrov, A. V. Khomenko, "Applications of the Priz light modulator", *Applied Optics*, 21, 21, (1982).

[8] J. Tjalling, "History of the newton-raphson method", *SIAM Review*, 37, 4, 1995.

[9] Li, C.-S., Zeng, Z.He, X.-L., "Optical voltage sensor using bismuth silicate crystal grown by hydrothermal method", *Journal of Optoelectronics Laser*, 25, 2, 2014.

[10] X. He, H. Zhou, W. Zhou, Z. Hu, C. Zhang, H. Huo, J. Wang, (...), F. Lu, "Solubility and optical activity of $Bi_{12}SiO_{20}$ crystals", *Journal of Crystal Growth*, 351, 1, 2012.

[11] Li, C., Cui, X., Yoshino, T. "Optical electric-power sensor by use of one bismuth germanate crystal", *Journal of Lightwave Technology*, 21, 5, 2003.

[12] A. R. Salazar, E. Jorge, J. E. Rueda, "Modification of the exchange of energy in BSO at equal optimized coupling constant", *Optics Communications* 212, 2002.

[13] M. Tebaldi, J. E. Rueda, N. Bolognini, "Talbot interferometer based on a birefringence grating", *Optics Communications* 185, 2000.

[14] J. E. Rueda, M. Tebaldi, S. Granieri, N. Bolognini, "Implementation of a photorefractive correlator based on a fake zoom lens", *Optik,* 113, 7, 2002.

[15] J. A. Gómez, H. G. Lorduy, A. Salazar, "Novel procedure for the simultaneous determination of the Debye length and electro-optic coefficient for an optically active BSO crystal", *Optics Communications,* 284, 460, 2011.

[16] J. A. Gómez, H. G. Lorduy, A. Salazar, "Improvement of the dynamic range of a fiber specklegram sensor based on volumen speckle recording in photorefractive materials", *Optics and Laser in Engineering*, 49, 473, 2011.

[17] J. A. Gómez, H. Lorduy, A. Salazar, "Influence of the volume speckle on fiber specklegram sensors based on four-wave mixing, Lorduy in photorefractive materials", *Optics Communications*, 284, 1008, 2011.

[18] J. E. Rueda, A. Romero, "Optical cryptography using Fresnel diffraction and phase conjugation", *Dyna*, 80, 181, 2013.

[19] V. H. Arístizabal, A. Hoyos, N. D. Gómez, J. A. Gómez, "Effect of Wavelength on Metrological Characteristics of Non-Holographic Fiber Specklegram Sensor", *Photonic Sensors*, 1, 1, 2015.

[20] A. Keshavarz, Z. Abbasi, "Spatial soliton pairs in an unbiased photovoltaic-photorefractive crystal circuit", *Spring*, 1, 1, 81, 2016.

[21] M. A. A. Khushaini, A.B-M.A. Ibrahim, "On the optical bistability of ferroelectrics via two-wave mixing: Beyond the slowly varying envelope approximation", *Optics Communications,* 381, 384, 2016.